PARAMETRIC ALGORITHMS TO EXTRACT ROOT TRAITS FOR BIOLOGY AND BIOMIMICRY

Thibaut Houette[1], Elena Stachew[1]
Claudia Naményi[1],
Jason W. Miesbauer[2], & Petra Gruber[1,3]

The study of tree root systems has been introduced in a biomimicry framework for engineering design because of current problems with soil instability due to urbanization, climate change, and the subsequent increase of extreme weather events affecting the built environment. Current civil and coastal infrastructures are static, limited by insertion techniques, monofunctional, and unable to adapt. In nature, root systems grow through various media as a dynamic, adaptive, multifunctional, and self-healing structure. Root systems' morphology can inform the design of multifunctional infrastructure.

The biomimicry transfer from root biology to technology is currently limited to generic morphological principles and strategies. Manual methods to measure and analyze root system architecture are labor-intensive and time-consuming, resulting in a lack of available data and difficulties when comparing results between studies. Recently, digital imaging techniques, including photogrammetry, are deployed to generate virtual 3D models of root systems.

Characterization of root system traits allows the abstraction and biomimicry transfer of specific root traits of interest (e.g., topology, surface-area-to-volume ratio, departure angle, tapering, porosity, curvature) to inform the design of architectural applications. Such characterization requires a standard method to measure root traits automatically, and reliably.

A parametric algorithm was developed with computational architectural tools, Rhinoceros and the plugin Grasshopper, to extract biological root traits of interest from virtual 3D models and find emerging patterns for biomimicry transfer. A skeletonization algorithm, developed in Grasshopper, extracts root system topology and associated architecture traits from 3D models of root systems. A manual step is needed to remove irregularities. Due to the large amount of root data exported, a brief statistical analysis follows to find emerging root morphology patterns. Finally, abstracted patterns will be applied to technical parametric designs toward multifunctional civil and coastal infrastructure.

This semi-automated process, extracting system architecture of biological tree roots from 3D models, not only serves the transfer of biological knowledge to technical applications, but allows for improved studies of root morphological traits in a systematic way, and potentially further investigations such as the adaptation of different species to various environments. Furthermore, it also showcases the potential of architectural tools for research on the morphologies of biological systems.

Keywords: Bioinspired design, parametric design, root research, civil engineering, coastal engineering.

1. INTRODUCTION

1.1. TOWARDS BIOMIMETIC CIVIL INFRASTRUCTURE INSPIRED BY ROOT SYSTEM ARCHITECTURE

With the continuous expansion of urban environments, ecosystem services once provided by natural environments are lost (Duraiappah et al. 2005; Grimm et al. 2008; McHale et al. 2015; McPhearson et al. 2016). The built environment should aim to provide the ecosystem services of the natural environment it replaces. For instance, cities produce impervious surfaces, and their stability relies on soil compaction. Soil compaction and impermeability compromise water storage and infiltration and so contribute to increased risks of flooding and erosion (Brown, Keath, and Wong 2009; Yang and Zhang 2011; Burns et al. 2012; Alaoui et al. 2018). Civil infrastructure is currently limited to monofunctional systems with simple morphologies, surface textures, and material choices, by the lack of accessibility, maintenance, and adaptation (Das 2007; Frost et al. 2017; Stachew, Houette, and Gruber 2021).

[1] Department of Biology,
The University of Akron, OH, USA
[2] The Morton Arboretum, IL, USA
[3] Transarch—Office for Transdisciplinary Research in Architecture, Ybbs, Austria

As a potential response to these limits, natural systems can serve as inspiration for the design of sustainable civil infrastructure. A variety of terms have been employed to describe the process of transferring biological knowledge to the fields of engineering, design, and architecture (i.e., bioinspiration, biomimetics, biomimicry, bionics, nature-based design) (ISO/TC 266 2015; Fayemi et al. 2017). In this paper, the term biomimicry serves to describe the method by which natural strategies and principles are analyzed, abstracted and applied to the sustainable designs of biomimetic foundation and coastal infrastructure. Well-known examples of biomimicry include the invention of VELCRO® (De Mestral 1961) from the morphology of burdock seeds and, for architecture, the passive ventilation of the Eastgate Center in Zimbabwe designed by Mick Pearce inspired by termite mounds (Turner and Soar 2008). Since biological and engineering contexts are very different in terms of scale, materials, manufacturing process, durability, and environment, the abstraction of principles is required for biomimicry transfer. Based on the understanding of the biological strategy, this abstraction can be performed at various levels, from form/organism to process/function to the ecosystem (Benyus 1997; Pawlyn 2011; Pedersen Zari 2012). In the research about tree root systems, the goal is to transfer morphological properties and processes towards the design of civil infrastructure to partially restore natural ecosystem services and functions.

In contrast to traditional civil infrastructure, root systems are multifunctional. They support the tree mechanically, explore soil media, uptake, store, and transport nutrients, prevent erosion, and create habitats. Root strategies of particular interest for the design of biomimetic civil infrastructure include self-penetrating tips, branched system increasing bearing area, enhanced friction through surface texture, integration of multifunctionality into individual components, self-healing processes, programmable decay, and dynamic adaptation to internal and external stimuli, especially in the wake of increasing urbanization and storm events. A comprehensive overview of root strategies of interest and analogies for civil infrastructure is presented in (Stachew, Houette, and Gruber 2021).

1.2. ROOT ANALYSIS TECHNIQUES

A deep understanding of root system principles and strategies is required for the abstraction and application of the design of civil infrastructure. Morphological tree root knowledge is limited due to the difficulty to visualize underground morphology, analyze complex architecture, and the high variation between species and environment (Waisel, Eshel, and Kafkafı 2002; Gyssels and Poesen 2003; Tamasi et al. 2005; Nicoll 2006; Danjon and Reubens 2008). Root traits have been analyzed through manual measurements in the field upon excavation entered in a program such as ArchiRoot (Dupuy 2007; www.archiroot.org.uk); or semi-automated processes manually entering root system data measured with an expensive field imaging tool (e.g. 3D digitizer) into a root analyzing software (e.g., AMAPmod (Godin, Caragilo, and Costes 1997)) using Multi-Tree Graph data as input (Danjon et al. 1999; Danjon and Reubens 2008) or CAD software such as Solidworks (Liang et al. 2017). These processes are tedious, time-consuming, and prone to user error, so it only allows researchers to gather a limited amount of root traits across an entire root system, which serves to answer a specific research question (Danjon and Reubens 2008). No standard procedure (e.g., similar to ASTM standards in material testing) has been developed to extract traits from root systems in a systematic way. The comparison of root system architectures across sites, species, and environments is therefore difficult since traits can be missing and extracting procedures are not standardized.

In response to these limitations, there is a push to apply advanced imaging systems for the analysis of 3D models. Various imaging devices are

used to generate models of root systems including Computed Tomography (CT)-scanners, terrestrial laser scanners, and ground-penetrating radars. The appropriate 3D imaging technique for a specific research project should be selected based on trade-offs between the following properties: accuracy, cost, ability to be performed in the field, accessibility, limitation from occlusion, and object size (Danjon and Reubens 2008). The complex morphology of root systems and occlusion caused by the roots, along with the soil, in visual imaging limit the application of those imaging techniques. Laser scanning and radar technologies can be used in the field but cannot detect occluded parts (Bucksch 2014) and require expensive equipment. X-ray, Magnetic Resonance Imaging, confocal microscopy, and Computed Tomography have the advantage of imaging elements through material such as soil or plant anatomy, but the specimen size is limited to small volumes imaged in a laboratory setting with expensive equipment (Fiorani et al. 2012; Kumi et al. 2015; van Dusschoten et al. 2016; Bucksch et al. 2017). In comparison, photogrammetry, also known as SFM-MVS (Structure from Motion and Multiple-View Stereophotogrammetry) has already been used to model coarse roots in the field at a low cost while preserving root system architecture (Morgenroth and Gomez 2014; Koeser et al. 2016; Miesbauer and Koeser 2019). While this technique does not require expensive equipment, it is still challenging to collect accurate morphological data from complex dense structures due to occluded parts. On the other hand, its accessibility facilitates standardized deployment across the globe to gather 3D models of diverse species adapted to various environments, which is the reasoning for choosing this technique for this project.

1.3. PARAMETRIC ALGORITHM FOR ROOT TRAIT EXTRACTION FROM 3D MODELS

This paper focuses on algorithmic abstraction and not on the photogrammetry process to obtain the 3D models nor the design of biomimetic infrastructure from the data extracted, which are topics of future publications. Similar to the imaging techniques, the analysis of root traits is currently performed manually or in a semi-automated manner which results in a time-consuming repetitive process, limiting the amount of collected data. In addition, most techniques cannot automatically gather both system topology and morphological traits, since they refer to different types of data and representations. The topology relates to the branching hierarchy of the root system. Morphological traits are characteristics of its form. In architecture and design, parametric plug-ins are often added to architectural software to perform actions more efficiently to a wide dataset (e.g., Grasshopper in Rhinoceros, Dynamo in Autodesk Revit). Such tools allow for repetitive analytic processes. The possibility to code in these parametric plug-ins allows users to go beyond the initial scope of the software and produce algorithms for various purposes.

Most morphological traits (i.e., length, diameter/radius, cross-section, orientation, departure angle, curvature) are based on root medial axes (i.e., centerlines), so the skeleton (i.e., collection of centerlines) of the root system needs to be generated (Danjon and Reubens 2008). 3D skeletonization processes have been of great interest to plant sciences, including the study of tree crowns, and root systems (Côté et al. 2009; Bucksch 2014). Main 3D skeletonization methods include: 3D Euclidean distance map (Nyström and Smedby 2001; Maddah, Hamid, and Afzali-Kusha 2003); Voronoi diagram (Näf et al. 1997); 3D thinning (Ma 1994; Ma and Sonka 1996; Palagyi 2008; She et al. 2009; Lohou 2010); and Reeb graph (Reeb 1946; Basiotti et al. 2008; Bucksch et al. 2010). The Reeb graph is of great interest for its robustness and potential for plant sciences most often utilized in plant sciences (Bucksch 2014). This concept

generates the centerline of an object by: cutting slices of that object following a given path (e.g., height of object); and connecting the centroids (i.e., geometric center point of a 2D shape) of each slice along that path. For simple objects (e.g., a cylinder), the slicing path can be defined following the linearity of the object. However, for complex 3D objects, the slicing path is not aligned with the centerline. For instance, when root branches or curves out, its centerline axis is at a different angle or blends in a curvature. As a result, slices following a single linear path over the entire geometry can no longer be perpendicular to the axes of all root components. One solution to this problem is to define slicing paths locally (Biasotti et al. 2008; Bucksch et al. 2010). However, these algorithms are developed in Python (developed by Guido van Rossum) or other coding languages without instantaneous feedback on a visual 3D representation, which makes them difficult to comprehend for non-experts and subsequently to adapt to specific case studies. Since the goal is to apply the abstracted knowledge to technical applications, the algorithm needs to be as comprehensive as possible for a wide range of users (i.e., both biologists and designers). Visual programming allows users to automatically visualize the outcome of each coding component in the 3D interface, which facilitates the comprehension and modification of algorithms by a wider audience while reducing user error through interactive visual assessment. The expertise on our team in visual programming was therefore leveraged to develop a 3D skeletonization algorithm in the visual programming language and interface, Grasshopper (by David Rutten at Robert McNeel & Associates) in the 3D modeling software, Rhinoceros (Robert McNeel & Associates, Seattle, WA, USA). Finally, the data extracted will be applied to technical systems through parametric design in Rhinoceros/Grasshopper. The development of the algorithms in the same software reduces the number of problems due to converting and transferring files between software and file types. In conclusion, a succession of parametric algorithms based on the Reeb graph was developed in Rhinoceros/Grasshopper to extract system topology and morphological traits of the root system architecture of 3D models generated from real root systems in the field through photogrammetry.

2. MATERIALS AND METHODS

2.1. DESCRIPTION OF MATERIALS

The root system model is from a 10-year-old Patmore green ash (Fraxinus pennsylvanica 'Patmore') tree which was processed as described in Koeser et al. (2016). The root system was excavated using a 244-cm (96-in.) hydraulic tree spade. Once harvested, the soil inside the root ball was removed using an air excavating tool (Airspade2000, Guardair Corporation, Chicopee, MA, USA), along with all roots less than 1-cm in diameter to reduce occlusion. The root system was then inverted and placed on a surface with paper-coded targets. A series of approximately 120 digital images was taken at distances of 1-2 meters all around the root system along three planes (i.e., slightly above, parallel to, and slightly below the root system), using a digital single-lens reflex camera (on a Nikon D7000 with an AF-S DX NIKKOR 12–24 mm f/4G lens, Nikon Corporation, Tokyo, Japan). A photogrammetry software (PhotoScan, Agisoft, LLC, St. Petersburg, Russia) was used to generate a 3D model of the root system from these images.

2.2. PARAMETRIC ALGORITHMS

The algorithm designed to extract morphological root traits is described in the following steps (Figure 1). First, traits pertaining to the overall root system morphology (i.e., volume, surface area, overall dimensions, porosity, 2D projections) are directly extracted from the 3D model and exported to a .csv file.

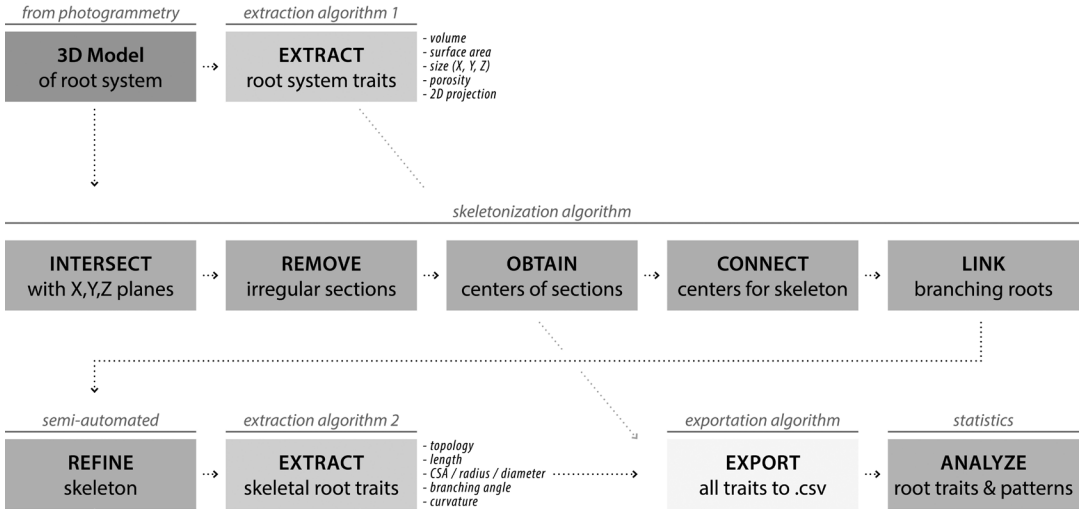

Figure 1: Workflow of the root trait extraction process performed in Rhinoceros with the Grasshopper plugin. CSA refers to cross-sectional area. Source: Author 2022.

Second, root centerlines (i.e., axes) are generated to extract system topology and morphological traits (i.e., length, diameter/radius, cross-section, orientation, departure angle, curvature). In this regard, the 3D model is skeletonized starting with intersecting the model with a number (e.g., 100) of equally spaced X, Y, Z planes to obtain random sections of the root systems along these planes (Figure 2-A). Depending on the roots' orientation in the 3D environment, those planes are not perpendicular to the root axes, resulting in incorrect centroids in cases where the deviation angle is too large. Therefore, the eccentricity of each intersection is computed and those with a major axis twice as long as the minor axis are automatically removed from the next steps of the algorithm (Figure 2-B). In this way, only the intersections in a plane closely aligned to the cross-section of the root are kept. In addition, some planes intersect a root at a branching location, resulting in sections with concave parts. To avoid highly incorrect centroid emergence, intersections containing concave parts are also automatically excluded. The centroids of the remaining sections (Figure 2-C) are connected through a looping algorithm generated with the plugin Octopus (by Robert Vierlinger), in Grasshopper. Starting from the trunk, the process connects each centroid (e.g., Point A) to its closest neighboring centroid (e.g., Point B). Once a centroid (i.e., Point B) is used, it becomes the next starting centroid (i.e., Point A) and is removed from the list of available neighbors (i.e., Points B). The loop stops when all points are connected. To avoid the reconnection of root tips with each other, line elements (i.e., connections between centroids) that are longer than a specified value, relating to the model's scale, are removed. The resulting collection of lines is then smoothed into curves (Figure 2-D).

Since the centerline curve stops at the last centroid identified (root tip in Figure 2-D), these curves' ends are elongated at their tip until they intersect the model's 3D surface. For the centerlines' base, the algorithm then connects branches together, which consists of several steps that extend each centerline at its base to find the intersection with their neighboring centerline (demonstrated in Figure 3).

The set of curves generated from this process represents the total 3D skeleton of the coarse root model. However, the process still results in inaccuracies in some centroids and resulting curves. Therefore, a manual step is required to adjust or delete some curves. In the manual refining process, the

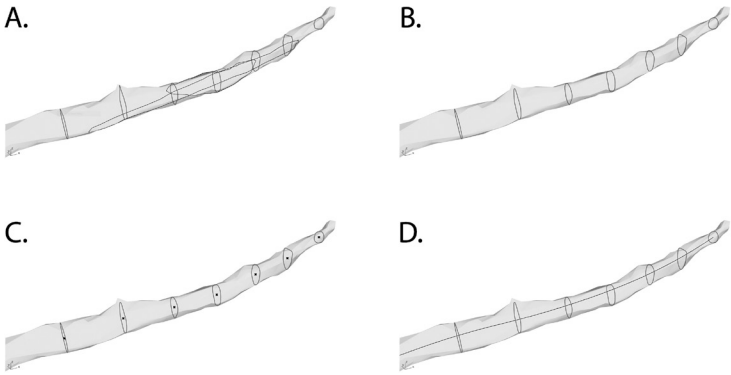

Figure 2: Screenshots of a root tip to show the main steps of the skeletonization algorithm in Rhinoceros with the Grasshopper plugin. First, the 3D model is intersected with 100 X, Y, and Z planes. Since the planes are not perpendicular to the root axes, the concavity and eccentricity of all sections is computed to find those with high eccentricity and concave elements (A), which are then automatically removed (B). Then, the centroids of each section are gathered (C) and connected through a looping algorithm to generate the centerline of the root (D). Source: Author 2022.

3D model is displayed together with the skeleton and serves as a reference for adjustments (Figure 4-B and C). These adjustments consist of deleting curves that still connect root tips (i.e., those with a length under the threshold given in the automated step), recentering curves along the centerline axis of the roots through manipulation of control points, and rectifying incorrect branching connections (i.e., moving the centerlines' intersection where they should be based on an understanding of biological branching connections). The 3D model and its current skeleton are saved as a separate file after each step to keep track of the process and manual edits (Figure 4). Despite the need to generate the entire skeleton of the root system to extract all morphological traits in relation to the system topology, this is not possible for the stump (i.e., region at the center of the root system immediately below the trunk). In its center, roots merge with their neighbors through secondary growth, so that the axes of individual roots are no longer identifiable. For a mature root system, roots' centerlines cannot be generated from a 3D model alone (Figure 4-D). To avoid the generation of an incorrect skeleton and mistakes in the resulting topology, the root centerlines stop at this stump region, when individual root axes can no longer be determined.

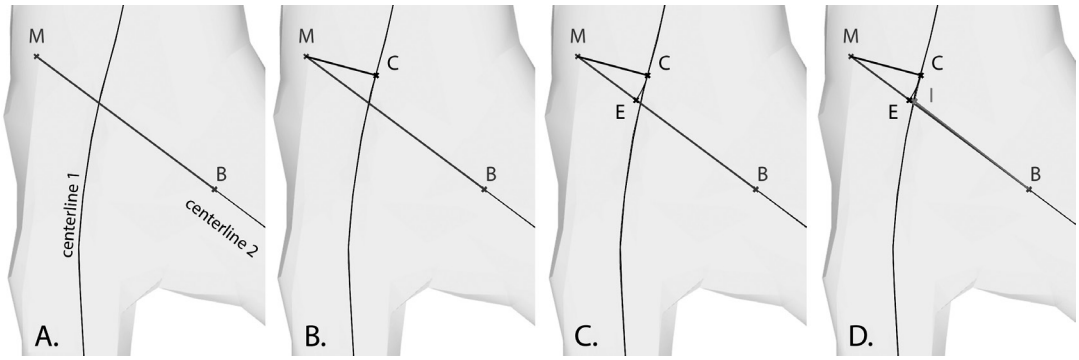

Figure 3: Diagram showing how the branches are connected to each other. Centerline 2, which needs to be connected to centerline 1, is extended at its base (Point B) until it intersects with the 3D surface of the mesh in point M (A). While this extension seems to intersect centerline 1 in a 2D view, both curves do not intersect in 3D. Therefore, the closest point to this intersection on the neighboring root centerline (Point C) is identified with a perpendicular projection (B). The distance from M to C is measured and removed from the previous curve extension to get Point E (C). Finally, the closest point to Point E on centerline 1 (Point I) is defined as the axes' intersection and is connected to the initial base of centerline 2 (Point B in D). Source: Author 2022.

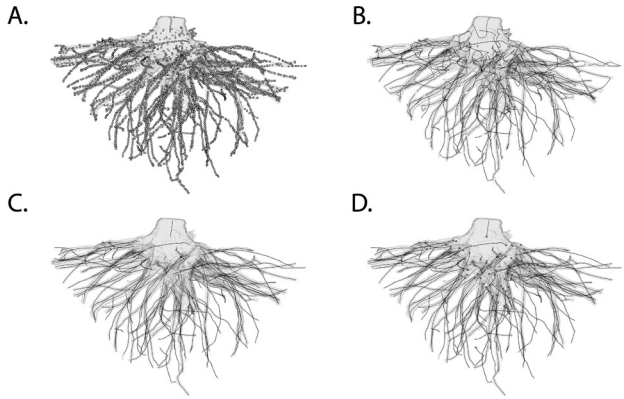

Figure 4: Screenshots of the 3D model of the root system throughout the skeletonization process: centroids generated (A), skeleton before manual revision (B), skeleton after manual revision (C), bases of roots which cannot be further connected in the stump area (D). Source: Author 2022.

After the skeletonization process, the skeleton, and more specifically each axis (i.e., centerline) serves as the basis to extract the second part of root traits (i.e., topology, length, diameter/radius, cross-section, orientation, departure angle, curvature). However, the root system's topology needs to be known to extract comparable morphological root trait data pertaining to specific roots within the system hierarchy. Four main types of topological ordering systems are used depending on the direction (i.e., centrifugal from base to root tips or centripetal from tips to base) and unit of ordering (i.e., segment or link): centrifugal link, centrifugal segment, centripetal link, centripetal segment (Berntson 1997). The centrifugal direction relates to the developmental growth of the roots, while centripetal corresponds to their functional aspect and physiology (Berntson 1997). The unit of ordering "segment" considers each root, from base to tip, as one topological order (e.g., the entire taproot being 0 in the centrifugal direction). This unit of ordering requires a clear understanding of which offspring is the continuation of the parent root, after a branching location. This can only be determined through judgment calls by researchers or growth analysis (Cannon 1949; Berntson 1997). When using "links" as the unit of ordering, the topological order changes at each branching location, resulting in a greater number of orders and subsequent higher resolution (Crawford and Young 1990). The centrifugal link system was selected for this algorithm for the following reasons. Links allow for comparison at branching locations. The centrifugal direction puts more emphasis on the structural roots and does not depend on finer roots. This topology is collected by identifying branching points, creating a hierarchy of topological orders, and assigning each root link to its corresponding order starting from the first parent root (Figure 5-B and C). The connectivity between root link centerlines is partly computed with the Sandbox Topology plugin (by tobesch)[1] in Grasshopper. Since the root system's center cannot be skeletonized accurately, the topological order of each root link emerging from the stump bulb was set to 0. To answer some biological questions, such as the relationship between the diameters of root links before and after branching, parent/offspring relationships are also required. Therefore, an additional part of the algorithm uses branching connections to assign a number to each root link based on its location within the root hierarchy. The name of each root link consists of the name of its parent root with an additional number, which makes each root link identifiable within the topological ordering system (Figure 5-D). At the end of the algorithm, root trait data is automatically exported to .csv files into a database from which statistical analysis is carried out to answer research questions.

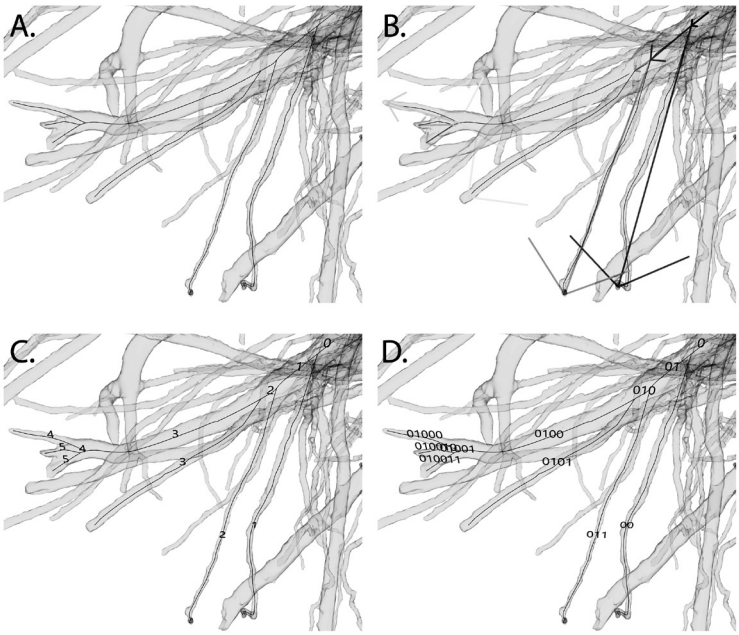

Figure 5: Screenshots of the topology and hierarchy of a selected root family (A). Topological orders shown through vectors (B) and numbering following the centrifugal link topological ordering system (C). To perform analyses of traits from parents to offspring, a name is given to each root link based on its location in the hierarchy (D). For example, root link "0" branches out into root link "00" and link "01" which then branches out into root links "010" and "011" (D). Source: Author 2022.

2.3. QUESTIONS TO BE ADDRESSED WITH EXTRACTED DATA

Once the algorithm exports root trait data to .csv files, it is statistically analyzed to answer specific research questions. With this type of morphological data, a wide range of research questions can be addressed for biomimicry transfer, as well as basic biological research, such as: How much tapering happens along a root link? How does the cross-section of a root vary along its length? How does the porosity of a root system differ between species and environments, such as along riverbanks?

Depending on the questions addressed, different types of statistical analysis are performed (Danjon and Reubens 2008). Examples include comparing specific traits between topological orders, quadrants (i.e., North, East, South, West), soil depths, distances from root center, or species and environment. To showcase the potential of this process, three main questions (one relating to biology, and two to biomimicry) are shown below. While root system trait abstraction for biomimicry transfer in the applications of architecture and engineering is the primary aim of this endeavor, the developed algorithm may also assist in answering questions related to furthering the understanding of the biology of root systems.

1. What is the ratio between the radius of a parent root and the sum of the radii of its offspring roots? This question comes from an interest in transport mechanisms and relates to the pipe model theory (Shinozaki et al. 1964; Lehnebach et al. 2018) and Murray's law (Murray 1926; McCulloh, Sperry, and Adler 2003).
2. What is the porosity of the root system and how does it vary per depth layer and distance from the trunk? This question provides insight regarding the formation of a soil-root plate, erosion prevention, and wave attenuation potential along coastlines for the design of

multifunctional civil and coastal infrastructure (Stachew, Houette, and Gruber 2021). Porosity is a significant geometrical parameter of aquatic vegetation ecosystems (e.g., seagrass beds, coral reefs, and mangrove forests) that influences bulk drag coefficient, subsequent flow attenuation, steady wake length development, and downstream velocity and turbulence responses (Nepf 1999; Lowe et al. 2007; Kazemi, Van de Riet, and Curet 2017).

3. What is the distribution of departure angles at branching locations? This question gives valuable insight for the bioinspired design of multifunctional hollow foundations, which can spread through larger volumes of soil, support structures, and transport resources through their centers.

2.4. EXTRACTION OF SPECIFIC ROOT TRAITS TO ADDRESS THE QUESTIONS SELECTED

To answer the first question about the ratio between the parent root's radius and the sum of the offspring's radii about the pipe model theory and Murray's law, the following data is exported from the algorithm to .csv files for each root link: topological order (e.g., 0, 1, 2), topological name (e.g., "0", "01", "010"), radius and cubed radius of the parent, radii and cubed radii of both offspring, and final ratios between parent and offspring radii or their cubed radii. The algorithm assesses the root system's hierarchy to compare the radius of each parent root to its two respective offspring roots. This ratio is calculated locally around each branching location and does not take the other root parts into consideration. Each virtual root link is cut by a perpendicular plane at its midpoint to collect the root's cross-section. The middle of each root link was chosen for the cutting plane since branching connections increase the thickness of each root link at its base and tip (Bucksch 2014). The average radius at this cross-section is then extracted and serves to compare each root. Twenty distinct root families (i.e., collection of roots descending from the same parent at topological order 0) with branching connections were selected throughout the entire root system to answer this question. Some cross sections are cutting through merged roots, due to local secondary growth or inaccuracy of the technique used to generate the virtual 3D model of the root system. These root links were removed from the analysis to only compare accurate data and extract reliable patterns.

To answer the second question, the root system's porosity was analyzed in 3 different ways: (1) volumetric porosity of the overall root system, (2) projection porosities in the X, Y, and Z directions, and (3) changes in sectional porosity across depth and distance from the trunk. Porosity is defined as the ratio of void space (i.e., soil particles and air between them) divided by the total space, which includes both void and solid space occupied by roots. This value is reported as a percentage. The porosity is calculated from the model's convex hull (i.e., the smallest convex shape that contains the entire 3D model) to follow its shape based on the excavation procedure (i.e., tree spade). The overall volumetric porosity of the root system is calculated by dividing the soil volume by the convex hull volume. The volume of soil equals the convex hull's volume minus the root system's volume. The projection porosities of the root system are also obtained from the surface area of the model projections in the X, Y, Z directions (i.e., 2D projection of 3D model on a plane following a specific direction) due to the researchers' interest in testing prototypes in these axial directions. For the sectional porosities throughout the soil depth, the 3D model is cut by horizontal planes every 10 cm. For the sectional porosities away from the trunk, the model is cut by concentric vertical cylinders of increasing radii, every 10 cm. In both cases, the surface area of these sections is then compared to the section of the convex hull at the same locations.

For the third question, the departure angles at each branching location are extracted from the same twenty root families used to answer the first question. The departure angle represents the branching angle between the two offspring centerlines of a parent root, measured 3 cm away from their branching location (or the entire offspring's length for links shorter than 3 cm long). This value was set because a longer distance would include root curvature while a smaller distance would integrate inaccuracies from root thickening at branching locations. The topological name of the parent root link serves as a reference for the location of each departure angle in the hierarchy.

3. RESULTS

3.1. ANALYSIS OF TRAITS TO ADDRESS THE BIOLOGICAL QUESTION

The distribution of ratios between the radius of each parent root link to the sum of the radii of its offspring (n = 21) follows a normal distribution with a mean of 93.00 ± 17.41% (Figure 6-A). It means that, on average, the radius of the parent root link is slightly smaller than the sum of the offspring root links. This ratio is not correlated with respect to topological orders (p-value = 0.0525, F1,19 = 4.2788) nor radius of parent (p-value = 0.8213, F1,19 = 0.0525). As expected, the parent radius is correlated with the sum of the offspring radii (p-value < 0.0001, F1,19 = 43.1651) (Figure 6-B). Concerning Murray's law, the ratio between the cubed radius of each parent to the sum of the cubed radii of its offspring shows a mean of 279.55 ± 190.21%. Murray's law predicts this ratio to be 100% for vascular systems (e.g., xylem in plants). Since our study considers the entire root cross-section, it seems logical that the ratio observed here does not equal 100%.

3.2. ANALYSIS OF TRAITS TO INFORM BIOMIMETIC DESIGN OF CIVIL INFRASTRUCTURE

For the transfer of root data toward biomimetic design, abstracted traits can be used. The shape and size of the root system that can be researched are contingent on the excavation technique (i.e., hydraulic tree spade in this case). The root system analyzed has a diameter of 2.02m and a height of 1.33m. The overall porosity of the root system equals 95.76% of the total volume (i.e., from the convex hull of the 3D model). The porosity along the X, Y, and Z projections respectively equals 47.80%, 43.33%, and 64.58% (Figure 7-A). The surface-to-volume ratio of this root system equals 79:1. The porosity throughout the root system's depth and distance from the trunk increases rapidly with increasing distance from the stump (Figure 7-B & C).

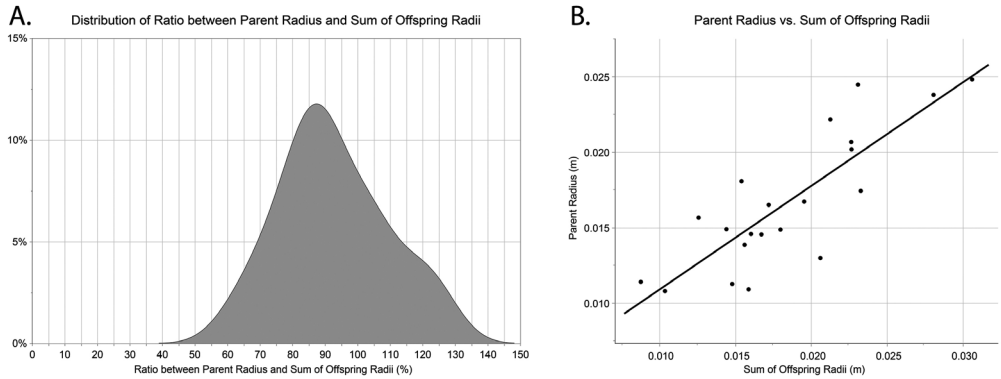

Figure 6: Distribution of the ratio between the parent radius and the offspring radii (A) and correlation between the parent radius and the sum of the offspring radii (fit-line, B). Source: Author 2022.

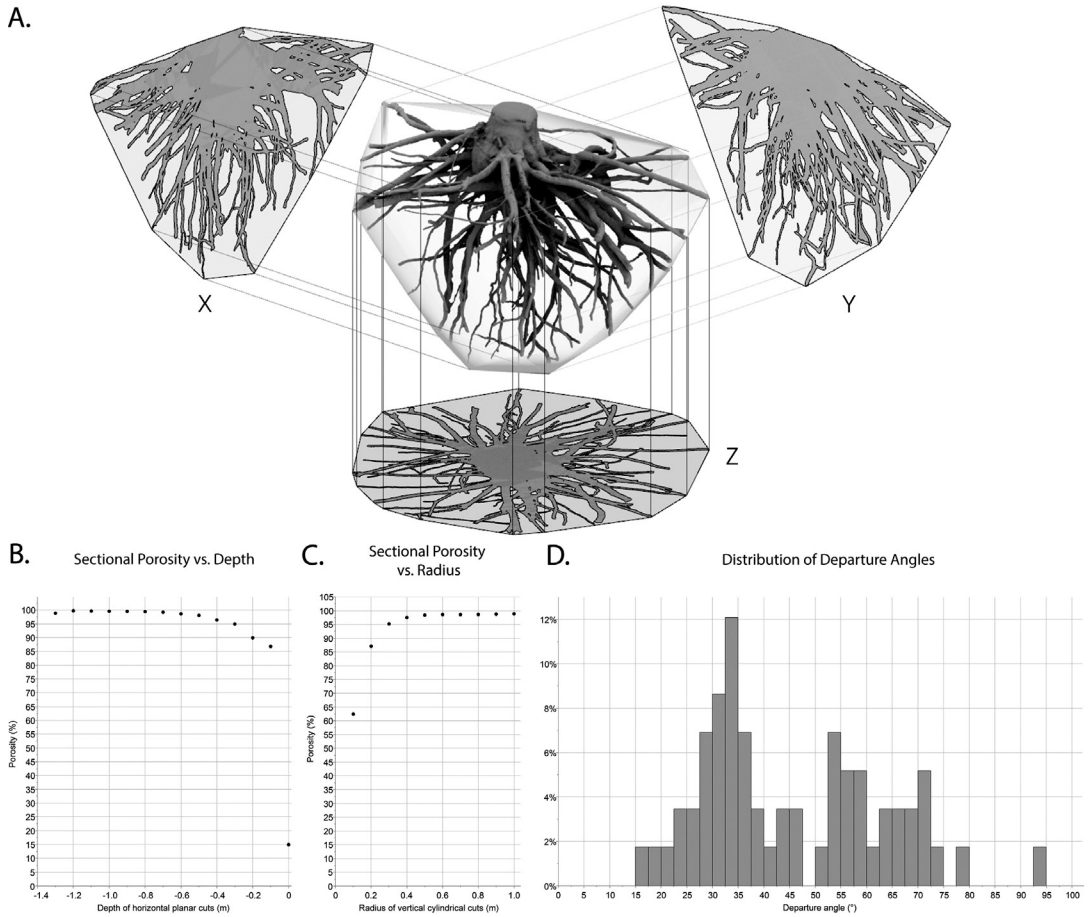

Figure 7: Shows the 3D model of the root system and its 2D projections in the X, Y and Z directions along with the 3D and 2D convex hulls used to calculate the different types of porosities (A), sectional porosity of the root system throughout its depth (B) and distance from the trunk center shown as the radius of each cylindrical cut (C), and the distribution of the departure angles throughout the root system (D). Source: Author 2022.

The distribution of departure angles (n = 56) throughout the root system showed peaks at approximately 33 degrees and 54 degrees, with an overall mean of 45.87 ± 17.38 degrees (Figure 7-D). The data shows no correlation between the departure angles and the topological order (p-value = 0.1968, F1,54 = 1.7082) nor the radius of parent root (p-value = 0.8453, F1,54 = 0.0384).

4. DISCUSSION AND CONCLUSION

4.1 ASSESSMENT OF ROOT TRAIT EXTRACTION ALGORITHMS

As described by Bucksch 2014, the extracted skeleton does not perfectly represent the actual plant network due to the limitation of the imaging technology. First, since the coarse roots in the root system's center (i.e., stump) merge together through secondary growth, it is not possible to reconstruct the complete plant network from the 3D model of the root system without making topological assumptions, tracking the root centerlines throughout time in 3D, or dissecting the roots to find growth patterns (Danjon and Reubens 2008). The lack of traceable morphology for this region of the root system means that the topological information cannot be derived. This impacts the entire root system's topology

and limits the comparison of root traits per topological order. In our analysis, the topological order of each root link emerging from the stump bulb was set to 0, but it is important to note that this apparent topological order does not correspond to the topological order of the actual growth process. This could be one reason for the absence of correlation between the root traits analyzed and the topological orders for this root system. Future research could focus on extracting the stump's topology and extracting the same data from other root systems to increase the number of data points and potentially identify emerging patterns.

Second, the extracted data's accuracy depends on the accuracy of the 3D model to be skeletonized and the limitations of the technique used to generate it. In the current case, photogrammetry is limited by occlusion, resulting in thicker roots, especially in the zone of rapid taper and at branching locations. Fine roots (i.e., under 1 cm in diameter) were lost and intentionally removed during the root excavation and preparation so that the data extracted from the 3D model only accounts for the coarse roots. For example, considering fine roots and root hairs would highly increase the surface area-to-volume ratio and decrease porosity. Fine roots amplify connectivity to soil particles and subsequently enhance erosion prevention (Reubens et al. 2007; Xiong et al. 2007; De Baets et al. 2020). Different excavation processes modify the root system's morphology in different ways. For instance, since roots are flexible and bend under mechanical loads (i.e., loads applied during excavation, soil/root removal, and gravity once the soil has been removed), traits related to the original orientation of the roots may need to be extracted from 3D models of roots imaged in their soil medium.

Five main requirements serve to assess skeletonization processes: (1) centerline location, (2) connected skeleton, (3) topology preservation, (4) thinnest skeleton possible and (5) independence from scaling, displacement, and rotation (Jiang et al. 2007; She et al. 2009). When considering the entire skeletonization process (i.e., including the manual refining step), all requirements are mostly satisfied. The current approach requires manual input to verify and adjust the centerline location (1). To improve the algorithm and reduce manual input, the centerlines generated with the current skeletonization algorithm could be used as local paths for orienting the cutting planes, similar to how contour lines of a mapping function can divide the complex model into local regions (Khromov and Mestetskiy 2012). Another iteration of the skeletonization algorithm would then use these paths to skeletonize each root in the system and connect their centerlines. However, similar problems will still occur, such as non-centeredness at branching locations. The connectivity (2) and topology (3) of the root system are preserved since the algorithm connects branches together at their branching location. The only exception to the connectivity and topology preservation is the stump, where topology cannot be determined. Therefore, parts of the skeleton are not connected. However, this limitation emerges from the characteristics of the root system and 3D model, not the skeletonization process. While traditional skeletonization methods are based on voxels and aim at the thinnest algorithm possible (i.e., 1-voxel thin) (She et al. 2009), our algorithm generates a vectorial centerline from a 3D mesh and is not constrained by the limitations of voxels (4). Finally, our process does not rely on scaling, displacement, and rotation (5) since the cutting planes and the rest of the algorithm use the boundary box of the root system model as a reference.

Once the skeleton has been generated and refined, morphological root traits and their place in the system topology are extracted for analysis. Therefore, research questions can be answered by comparing both data types and their effects on each other, such as the decrease in diameter from one topological order to the next. The results section shows how topology serves to answer specific biological or biomimicry questions.

4.2. COLLECTION OF ROOT TRAITS TO STUDY ADAPTATION ACROSS SPECIES AND ENVIRONMENTS

This algorithm extracts system topology and morphological root traits from 3D models in a systematic process. Extracting traits from accurate 3D models of root systems allows for research questions to be answered long after the 3D model has been generated. In addition, a standard root analysis process facilitates the data comparison between studies and the subsequent emergence of trends. The large amount of root trait data extracted from each root model can feed a database, such as the Fine-Root Ecology Database (FRED) (Iversen et al. 2017) or the Digital Imaging of Root Traits (DIRT) (Das et al. 2015). Similar to the 3D models, the database can act as a storage of root knowledge for future research questions. Root models from around the globe could be analyzed with this standard process to produce a wide set of comparable data. Broader questions, such as the adaptation of different tree species to different environments, could therefore be addressed.

4.3. TRANSFER OF ROOT KNOWLEDGE TO BIOMIMETIC DESIGN

For the design of biomimetic civil infrastructure, specific root traits are relevant for different related functions. Therefore, the functions of interest dictate the type of root trait to be extracted from the root model. For instance, the distribution of departure angles in root systems can inform the morphology of branched building foundations to optimize their spread throughout the soil media for structural support and erosion prevention. For example, a vertical pile branching into multiple offspring following a small departure angle allows it to reach deeper soil layers, as the offspring's orientation remains similar to the parent. A pile branching with a larger departure angle would greatly modify the offspring's orientation and could, for instance, serve to increase the bearing area. Furthermore, the surface-to-volume ratio of the root system analyzed equals 79:1. In comparison, a traditional pipe foundation with a 50-cm diameter and 10-m depth has a surface area-to-volume ratio of 8:1. In both cases, only the surface area in contact with the soil is taken into account (i.e., not the cross-sectional area of the trunk or pile at the soil surface). A higher surface-to-volume ratio means that for an equal volume of foundation material, a wider volume of soil is recruited to transfer structural loads (i.e., larger bearing and frictional area), or exchange resources. This high surface-to-volume ratio is also reflected in the porosity results which can provide valuable insight for structural support, erosion prevention, and natural habitat creation. Volumetric porosity, in addition to other root traits such as diameter, tapering, and departure angle that influence the size, structure, and distribution of open areas along the dimensions of the root system, can be tested to understand their singular and interactive effects on downstream flow and turbulence responses, affecting wave attenuation and erosion performance. For example, porosities of traditional coastal protection revetment structures such as concrete block, porous concrete block, and ecological concrete vary from 15-40% (Chen, Xu, and Ying 2016), while the overall volumetric porosity of the root system analyzed is 96%. In lab studies where vegetation is often modeled as an array of rigid, vertical cylinders of the same diameter and spacing (Chen et al. 2012; Zong and Nepf 2012), the geometric parameters are assumed to be equivalent throughout the length, width, and depth of the vegetative region. However, spacing between individual elements along the dimensions of a coastal structure can be varied to create habitat by targeting the preferred flow and energy regimes of native fish species (Hockley et al. 2014; Kerr et al. 2021). Variations in sectional and projection porosities in the root system analyzed (Figure 7) provide additional geometrical parameters and possibilities for localized habitat creation, wave

attenuation, and coastal erosion reduction performance.

In addition to extracting root traits to inform a desired function, transferring and integrating abstracted root strategies and principles can also lead to concepts and designs of multifunctional adaptive root-inspired infrastructure, which have been explored in Stachew, Houette, and Gruber (2021). Since root systems and civil infrastructure do not exist in the same context (in terms of scale, materials, environment, and requirements), the efficiency of the transferred traits and resulting designs will be evaluated through extensive prototyping testing. These tests could then, in a process called reverse biomimetics (VDI 6220 2012), also serve to learn more about the biological role model itself.

CONCLUSION

In response to the current limitations of civil infrastructure, especially with the need for sustainability and to address the increasing stress of climate change, the biomimicry transfer of root strategies, principles, and traits offers an avenue for the design of multifunctional adaptive civil infrastructure. In the analysis of root system architecture, root traits need to be extracted in a systematic way to be comparable between studies. The focus of this paper is to present a semi-automated algorithm to extract traits from 3D models of root systems, in a visual programming language and 3D interface to facilitate its comprehension and usability by researchers and practitioners. The algorithm is skeletonizing root systems' 3D models based on the Reeb graph. A manual step is required to adjust skeleton inaccuracies. The skeleton is the basis to extract morphological root traits and system topology, which serves to answer both biological questions and inform the design of root-inspired infrastructure. This root analysis process allows for answering emerging research questions long after the 3D model has been generated. Future research could aim at improving the algorithm with machine learning, feeding the extracted root traits into databases, and continuing to evaluate and integrate these abstracted traits for the design of civil infrastructure.

ACKNOWLEDGEMENTS

The authors would like to thank Dr. Andrew Koeser for the 3D model of the green ash root system which was generated with photogrammetry in Koeser et al., 2016, Dr. Henry Astley for his advice on coding complex algorithms and Dr. Randall Mitchell for his guidance with the statistical analysis.

ENDNOTES

1 Plugin available on food4Rhino which hosts grasshopper plugins: https://www.food4rhino.com/en/app/sandbox-topology

REFERENCES

Alaoui, A., Rogger, M., Peth, S., and Blöschl, G. 2018. "Does Soil Compaction Increase Floods? A Review." *Journal of Hydrology* 355. Elsevier B.V. https://doi.org/10.1016/j.jhydrol.2017.12.052.

Baets, S. De, Denbigh, T. D. G., Smyth, K. M., Eldridge, B. M., Weldon, L., Higgins, B., Matyjaszkiewicz, A. et al. 2020. "Micro-Scale Interactions between Arabidopsis Root Hairs and Soil Particles Influence Soil Erosion." *Communications Biology* 3 (1): 164. https://doi.org/10.1038/s42003-020-0886-4.

Benyus, J. M. 1997. *Biomimicry: Innovation Inspired by Nature*. Harper Perennial.

Berntson, G. M. 1997. "Topological Scaling and Plant Root System Architecture: Developmental and Functional Hierarchies." *New Phytologist* 135: 621–34.

Biasotti, S., Giorgi, D., Spagnuolo, M., and Falcidieno, B. 2008. "Reeb Graphs for Shape Analysis and Applications." *Theoretical Computer Science* 392 (1–3): 5–22. https://doi.org/10.1016/J.TCS.2007.10.018.

Brown, R. R., Keath, N., and Wong, T. H. F. 2009. "Urban Water Management in Cities: Historical, Current and Future Regimes." *Water Science and Technology* 59 (5): 847–55. https://doi.org/10.2166/wst.2009.029.

Bucksch, A. 2014. "A Practical Introduction to Skeletons for the Plant Sciences." *Applications in Plant Sciences* 2 (8): 1400005. https://doi.org/10.3732/apps.1400005.

Bucksch, A., Atta-Boateng, A., Azihou, A. F., Battogtokh, D., Baumgartner, A., Binder, B. M., Braybrook, S. A., et al. 2017. "Morphological Plant Modeling: Unleashing Geometric and Topological Potential within the Plant Sciences." *Frontiers in Plant Science* 8. https://doi.org/10.3389/fpls.2017.00900.

Bucksch, A., Lindenbergh, R., and Menenti, M. 2010. "SkelTre." *The Visual Computer* 26 (10): 1283–1300. https://doi.org/10.1007/S00371-010-0520-4.

Burns, M. J., Fletcher, T. D., Walsh, C. J., Ladson, A. R., and Hatt, B. E. 2012. "Hydrologic Shortcomings of Conventional Urban Stormwater Management and Opportunities for Reform." *Landscape and Urban Planning* 105 (3): 230–40. https://doi.org/10.1016/j.landurbplan.2011.12.012.

Cannon, W. A. 1949. "A Tentative Classification of Root Systems." *Ecology* 30 (4): 542–48. https://doi.org/10.2307/1932458.

Chen, Y., Xu, S., and Jin, Y. 2016. "Evaluation on Ecological Restoration Capability of Revetment in Inland Restricted Channel." *KSCE Journal of Civil Engineering* 20 (6): 2548–58. https://doi.org/10.1007/s12205-015-0291-6.

Chen, Z., Ortiz, A., Zong, L., and Nepf, H. 2012. "The Wake Structure behind a Porous Obstruction and Its Implications for Deposition near a Finite Patch of Emergent Vegetation." *Water Resources Research* 48 (9). https://doi.org/10.1029/2012WR012224.

Côté, J. F., Widlowski, J. L., Fournier, R. A., and Verstraete, M. M. 2009. "The Structural and Radiative Consistency of Three-Dimensional Tree Reconstructions from Terrestrial Lidar." *Remote Sensing of Environment* 113 (5): 1067–81. https://doi.org/10.1016/J.RSE.2009.01.017.

Crawford, J. W., and Young, I. M. 1990. "A Multiple Scaled Fractal Tree." *Journal of Theoretical Biology* 145 (2): 199–206. https://doi.org/10.1016/S0022-5193(05)80125-0.

Danjon, F., and Reubens, B. 2008. "Assessing and Analyzing 3D Architecture of Woody Root Systems, a Review of Methods and Applications in Tree and Soil Stability, Resource Acquisition and Allocation." *Plant and Soil* 303: 1-34. https://doi.org/10.1007/s11104-007-9470-7.

Danjon, F., Sinoquet, H., Godin, C., Colin, F., and Drexhage, M. 1999. "Characterisation of Structural Tree Root Architecture Using 3D Digitising and AMAPmod Software." *Plant and Soil* 211 (2): 241–58. https://doi.org/10.1023/A:1004680824612.

Das, A., Schneider, H., Burridge, J., Ascanio, A. K. M., Wojciechowski, T., Topp, C. N., Lynch, J. P., Weitz, J. S., and Bucksch, A. 2015. "Digital Imaging of Root Traits (DIRT): A High-Throughput Computing and Collaboration Platform for Field-Based Root Phenomics." *Plant Methods* 11 (1): 1–12. https://doi.org/10.1186/S13007-015-0093-3.

Das, B. M. 2007. *Principles of Foundation Engineering. 6th edition*. Florence, KY, United States: Cengage Learning, Inc.

Duraiappah, A. K., Naeem, S., Agardy, T., Ash, N. J., Cooper, H. D., Diaz, S., Faith, D. P., et al. 2005. *Ecosystems and Human Well-Being: Biodiversity Synthesis; a Report of the Millennium Ecosystem Assessment*. Washington DC., United States: World Resources Institute.

Dusschoten, D. van, Metzner, R., Kochs, J., Postma, J. A., Pflugfelder, D., Buehler, J., Schurr, U., and Jahnke, S. 2016. "Quantitative 3D Analysis of Plant Roots Growing in Soil Using Magnetic Resonance Imaging." *Plant Physiology* 170. https://doi.org/10.1104/pp.15.01388.

Fayemi, P.-E., Wanieck, K., Zollfrank, C., Maranzana, N., and Aoussat, A. 2017. "Biomimetics: Process, Tools and Practice." *Bioinspiration and Biomimetics* 12 (1). https://doi.org/10.1088/1748-3190/12/1/011002.

Fiorani, F., Rascher, U., Jahnke, S., and Schurr, U. 2012. "Imaging Plants Dynamics in Heterogenic Environments." *Current Opinion in Biotechnology* 23 (2): 227–35. https://doi.org/10.1016/j.copbio.2011.12.010.

Frost, J. D., Martinez, A., Mallett, S. D., Roozbahani, M. M., and DeJong, J. T. 2017. "Intersection of Modern Soil Mechanics with Ants and Roots." In *Geotechnical Special Publication, 900–909. American Society of Civil Engineers (ASCE)*. https://doi.org/10.1061/9780784480472.096.

Godin, C., Caraglio, Y., and Costes, E. 1997. "Exploring Plant Topological Structure with the AMAPmod Software: An Outline." *Silva Fennica* 31 (3): 357–68. https://doi.org/10.14214/SF.A8533.

Grimm, N. B., Faeth, S. H., Golubiewski, N. E., Redman, C. L., Wu, J., Bai, X., and Briggs, J. M. 2008. "Global Change and the Ecology of Cities." *Science 319* (5864): 756-60. https://doi.org/10.1126/science.1150195.

Gyssels, G., and Poesen, J. 2003. "The Importance of Plant Root Characteristics in Controlling Concentrated Flow Erosion Rates." *Earth Surface Processes and Landforms* 28 (4): 371–84. https://doi.org/10.1002/esp.447.

Hockley, F. A., Wilson, C. A. M. E., Brew, A., and Cable, J. 2014. "Fish Responses to Flow Velocity and Turbulence in Relation to Size, Sex and Parasite Load." *Journal of the Royal Society Interface* 11 (91). https://doi.org/10.1098/rsif.2013.0814.

International Organization for Standardization / TC 266. 2015. "ISO 18458:2015 Biomimetics -- Terminology, Concepts and Methodology," 1–6. https://www.iso.org/standard/62500.html.

Iversen, C. M., McCormack, M. L., Powell, A. S., Blackwood, C. B., Freschet, G. T., Kattge, J., Roumet, C., et al. 2017. "A Global Fine-Root Ecology Database to Address below-Ground Challenges in Plant Ecology." *New Phytologist* 215 (1): 15–26. https://doi.org/10.1111/nph.14486.

Jiang, Z., Wu, K., Couples, G., Van Dijke, M. I. J., Sorbie, K. S., and Ma, J. 2007. "Efficient Extraction of Networks from Three-Dimensional Porous Media." *Water Resources Research* 43 (12): 12–15. https://doi.org/10.1029/2006WR005780.

Kazemi, A., Van de Riet, K., and Curet, O. M. 2017. "Hydrodynamics of Mangrove-Type Root Models: The Effect of Porosity, Spacing Ratio and Flexibility." *Bioinspiration and Biomimetics* 12 (5): 056003. https://doi.org/10.1088/1748-3190/aa7ccf.

Kerr, J. R., Vowles, A. S., Crabb, M. C., and Kemp, P. S. 2021. "Selective Fish Passage: Restoring Habitat Connectivity without Facilitating the Spread of a Non-Native Species." *Journal of Environmental Management* 279: 110908. https://doi.org/10.1016/j.jenvman.2020.110908.

Khromov, D., and Mestetskiy, L. 2012. "3D Skeletonization as an Optimization Problem." In *24th Canadian Conference on Computational Geometry. Charlottetown*, August 8-10.

Koeser, A. K., Roberts, J. W., Miesbauer, J. W., Lopes, A. B., Kling, G. J., Lo, M., and Morgenroth, J. 2016. "Testing the Accuracy of Imaging Software for Measuring Tree Root Volumes." *Urban Forestry and Urban Greening* 18: 95–99. https://doi.org/10.1016/j.ufug.2016.05.009.

Kumi, F., Han Ping, M. P., Jian Ping, H. P., and Ullah, I. 2015. "Review of Applying X-Ray Computed Tomography for Imaging Soil-Root Physical and Biological Processes." *International Journal of Agricultural and Biological Engineering* 8 (5): 1–14. https://doi.org/10.3965/j.ijabe.20150805.1490.

Lehnebach, R., Beyer, R., Letort, V., and Heuret, P. 2018. "The Pipe Model Theory Half a Century on: A Review." *Annals of Botany* 121: 773–95. https://doi.org/10.1093/aob/mcx194.

Liang, T., Knappett, J. A., Bengough, A. G., and Ke, Y. X. 2017. "Small-Scale Modelling of Plant Root Systems Using 3D Printing, with Applications to Investigate the Role of Vegetation on Earthquake-Induced Landslides." *Landslides* 14 (5): 1747–65. https://doi.org/10.1007/s10346-017-0802-2.

Lohou, C. 2010. "Detection of the Non-Topology Preservation of Ma and Sonka's Algorithm, by the Use of P-Simple Points." *Computer Vision and Image Understanding* 114 (3): 384–99. https://doi.org/10.1016/J.CVIU.2009.10.003.

Lowe, R. J., Falter, J. L., Koseff, J. R., Monismith, S. G., and Atkinson, M. J. 2007. "Spectral Wave Flow Attenuation within Submerged Canopies: Implications for Wave Energy Dissipation." *Journal of Geophysical Research: Oceans* 112 (C5). https://doi.org/10.1029/2006JC003605.

Ma, C. M. 1994. "On Topology Preservation in 3D Thinning." *CVGIP: Image Understanding* 59 (3): 328–39. https://doi.org/10.1006/CIUN.1994.1023.

Ma, C. M., and Sonka, M. 1996. "A Fully Parallel 3D Thinning Algorithm and Its Applications." *Computer Vision and Image Understanding* 64 (3): 420–33. https://doi.org/10.1006/CVIU.1996.0069.

Maddah, M., Soltanian-Zadeh, H., and Afzali-Kusha, A. 2003. "Snake Modeling and Distance Transform Approach to Vascular Centerline Extraction and Quantification." *Computerized Medical Imaging and Graphics* 27 (6): 503–12. https://doi.org/10.1016/S0895-6111(03)00040-5.

McCulloh, K. A., Sperry, J. S. and Adler, F. R. 2003. "Water Transport in Plants Obeys Murray's Law." *Nature* 2003 421:6926 421 (6926): 939–42. https://doi.org/10.1038/nature01444.

McHale, M. R., Pickett, S. T. A., Barbosa, O., Bunn, D. N., Cadenasso, M. L., Childers, D. L., Gartin, M., et al. 2015. "The New Global Urban Realm: Complex, Connected, Diffuse, and Diverse Social-Ecological Systems." *Sustainability* 7 (5): 5211–40. https://doi.org/10.3390/su7055211.

McPhearson, T., Haase, D., Kabisch, N., and Gren, Å. 2016. "Advancing Understanding of the Complex Nature of Urban Systems." *Ecological Indicators*, Navigating Urban Complexity: Advancing Understanding of Urban Social – Ecological Systems for Transformation and Resilience, 70: 566–73. https://doi.org/10.1016/j.ecolind.2016.03.054.

Mestral, G. De. 1961. Separable Fastening Device. U.S. Patent No. 3,009,235.

Miesbauer, J. W., and Koeser, A. K. 2019. "The Development of 3-D Imaging Technologies to Measure Root Volume and Assess Stability." In *The Landscape Belowground IV: Proceedings of an International Workshop on Tree Root Development in Urban Soils*: 332-355. International Society of Arboriculture.

Morgenroth, J., and Gomez, C. 2014. "Assessment of Tree Structure Using a 3D Image Analysis Technique-A Proof of Concept." *Urban Forestry and Urban Greening* 13 (1): 198–203. https://doi.org/10.1016/j.ufug.2013.10.005.

Murray, C. 1926. "The Physiological Principle of Minimum Work: I. The Vascular System and the Cost of Blood Volume." *Proceedings of the National Academy of Sciences* 12 (3): 207–14. https://doi.org/10.1073/PNAS.12.3.207.

Näf, M., Székely, G., Kikinis, R., Shenton, M. E., and Kübler, O. 1997. "3D Voronoi Skeletons and Their Usage for the Characterization and Recognition of 3D Organ Shape." *Computer Vision and Image Understanding* 66 (2): 147–61. https://doi.org/10.1006/CVIU.1997.0610.

Nepf, H. M. 1999. "Drag, Turbulence, and Diffusion in Flow through Emergent Vegetation." *Water Resources Research* 35 (2): 479–89. https://doi.org/10.1029/1998WR900069.

Nicoll, B. C. 2006. "Effects of Soil, Terrain and Wind Climate on Tree Root System Development and Anchorage." PhD diss., The University of Edinburgh.

Nyström, I., and Smedby, Ö. 2001. "Skeletonization of Volumetric Vascular Images—Distance Information Utilized for Visualization." *Journal of Combinatorial Optimization* 5 (1): 27–41. https://doi.org/10.1023/A:1009829415835.

Palágyi, K. 2008. "A 3D Fully Parallel Surface-Thinning Algorithm." *Theoretical Computer Science* 406 (1–2): 119–35. https://doi.org/10.1016/J.TCS.2008.06.041.

Pawlyn, M. 2011. *Biomimicry in Architecture*. London: RIBA Publishing.

Reeb, G. 1946. "Sur Les Points Singuliers d'une Forme de Pfaff Complètement Intégrable Ou d'une Fonction Numérique." *Comptes Rendus Acad. Sciences* 222: 847–49. https://ci.nii.ac.jp/naid/10024635920.

Reubens, B., Poesen, J., Danjon, F., Geudens, G., and Muys, B. 2007. "The Role of Fine and Coarse Roots in Shallow Slope Stability and Soil Erosion Control with a Focus on Root System Architecture: A Review." *Trees - Structure and Function* 21 (4): 385–402. https://doi.org/10.1007/s00468-007-0132-4.

She, F. H., Chen, R. H., Gao, W. M., Hodgson, P. D., Kong, L. X., and Hong, H. Y. 2009. "Improved 3D Thinning Algorithms for Skeleton Extraction." In *DICTA 2009 - Digital Image Computing: Techniques and Applications*, 14–18. https://doi.org/10.1109/DICTA.2009.13.

Shinozaki, K., Yoda, K., Hozumi, K., and Kira, T. 1964. "A Quantitative Analysis of Plant Form-the Pipe Model Theory: I. Basic Analyses." *Japanese Journal of Ecology* 14 (3): 97–105. https://doi.org/10.18960/SEITAI.14.3_97.

Stachew, E., Houette, T., and Gruber, P. 2021. "Root Systems Research for Bioinspired Resilient Design: A Concept Framework for Foundation and Coastal Engineering." *Frontiers in Robotics and AI* 8: 109. https://doi.org/10.3389/frobt.2021.548444.

Tamasi, E., Stokes, A., Lasserre, B., Danjon, F., Berthier, S., Fourcaud, T., and Chiatante, D. 2005. "Influence of Wind Loading on Root System Development and Architecture in Oak (Quercus Robur L.) Seedlings." *Trees* 19 (4): 374–84. https://doi.org/10.1007/s00468-004-0396-x.

Turner, S. J., and Soar, R. C. 2008. "Beyond Biomimicry: What Termites Can Tell Us about Realizing the Living Building." In *Proceedings of 1st International Conference on Industrialized, Intelligent Construction*. Loughborough University, May 14-16.

VDI 6220. 2012. "Biomimetics—conception and strategy—differences between biomimetic and conventional methods/products." *VDI-Richtlinien* (Berlin: Beuth)

Waisel, Y., Eshel, A., and Kafkafi, U. 2002. *Plant Roots - the Hidden Half*. 3rd ed. Basel, New York: Marcel Dekker. https://doi.org/10.1093/aob/mcf252.

Xiong, Y.-M., Xia, H.-P., Li, Z.-A., and Cai, X.-A. 2007. "Effects and mechanisms of plant roots on slope reinforcement and soil erosion resistance: a research review." *Ying Yong Sheng Tai Xue Bao = The Journal of Applied Ecology* 18 (4): 895–904.

Yang, J. L., and Zhang, G. L. 2011. "Water Infiltration in Urban Soils and Its Effects on the Quantity and Quality of Runoff." *Journal of Soils and Sediments* 11 (5): 751–61. https://doi.org/10.1007/s11368-011-0356-1.

Zari, M. P. 2012. "Ecosystem Services Analysis for the Design of Regenerative Urban Built Environments." PhD diss., Victoria University of Wellington.

Zong, L., and Nepf, H. 2012. "Vortex Development behind a Finite Porous Obstruction in a Channel." *Journal of Fluid Mechanics* 691: 368–91. https://doi.org/10.1017/jfm.2011.479.